PARTIAL SPHERE TRANSDUCERS

P R BRAZIER-SMITH

PLESSEY MARINE - TEMPLECOMBE

The electroacoustic performance of partial sphere transducers has been examined experimentally and a theory postulated for their design. The theory for the ceramic/support interaction has been applied to specific design configurations of partial sphere transducers and checked against practical measurements. The results indicate that practical partial sphere transducers are feasible, and that the ceramic/support interaction theory is valid.

Since the initial study, further theoretical work has been carried out on the prediction of certain parameters of partial sphere transducers.

Using the theory of Kalnins (1964), a method has been developed to deduce the modes of an axisymmetric partial spherical shell given the static stiffness of the shell support. The mode shapes and frequencies are calculated for an 'in vacuo' state. The effect of water loading on the shell is then examined, and the change of resonant frequency, the power emitted and the beam patterns are calculated. These techniques exist as computer software and have been validated against an experimental transducer.

The theoretical performance of a particular partial spherical shell transducer is assessed using a suite of five computer programs. These calculate the modal frequencies and mode shapes in vacuo, the total radiated power and modal amplitudes in water for a range of frequencies, and the beam pattern in the form of the far field pressure distribution for any selected frequency.

The input data required for the suite comprises detail of the spherical shell geometry, the static stiffness of the supports, and the frequency range over which the analysis is required.

The static support stiffnesses are obtained using the finite element analysis (PAFEC suite of programs). The ceramic support is modelled as a series of elemental shapes, and the program suite calculates the displacements of the support for a given set of input forces. These are separated into the horizontal and vertical stiffnesses and the bending stiffness of the support structures.

Introduction

The vibration of spherical shells has been studied by a number of authors. Notably, Kalnin's (1964) described how the axisymmetric modes of a partial spherical cap may be determined for a range of simple boundary conditions. Sonstegard (1969) and more recently Lou and Su (1978) consider the effect of fluid on axisymmetric vibrations of a complete spherical shell.

The present work extends the work of Kalnins to incorporate more complex boundary conditions of a compliant mounting attached to the edge of the shell. Also the effect of fluid loading is considered on the basis that the shell was mounted in a matching spherical baffle.

Frequencies and Shapes of Modes in Vacuo

Consider the shell geometry as illustrated in Figure 1.

R is the shell radius, h is the shell thickness, ϕ_0 is the semicap angle and ϕ is a general angle. If W an U represent displacements of the shell in normal and tangential direction, then for periodic motion, these can be written in terms of amplitudes:

$$\left.\begin{aligned} W &= \hat{W} e^{i\omega t} \\ U &= \hat{U} e^{i\omega t} \end{aligned}\right\} \quad \ldots\ldots\ldots (1)$$

(note: the 'hats' shall indicate amplitudes throughout)

From Kalnins (1964), mode shapes conform to the following:

$$\hat{W} = \sum_{\alpha=1}^{3} A_\alpha P_{n_\alpha}(\cos\phi) \qquad \ldots\ldots\ldots (2)$$

$$\hat{U} = -\sum_{\alpha=1}^{3} (1+\nu) C_\alpha A_\alpha P'_{n_\alpha}(\cos\phi) \qquad \ldots\ldots\ldots (3)$$

Where P_{n_α} and P'_{n_α} are respectively the Legendre and associated Legendre functions of order zero and degree n_α and:

$$C_\alpha = \frac{1 + (\lambda_\alpha - 2)/[(1+\nu)(1+\xi)}{1 - \nu - \lambda_\alpha + \xi(1-\nu^2)\Omega^2/(1+\xi)}$$

$$n_\alpha = -0.5 + (0.25 + \lambda_\alpha)^{1/2}$$

$$\xi = 12R^2/h^2$$

$$\Omega^2 = \rho\omega^2 R^2/E$$

ω is the angular eigen frequency, E, ρ and ν are respectively Young's modulus, density and Poisson's ratio. A_α are chosen so that the specified boundary conditions are satisfied.

The dimensionless numbers λ_α are the solutions of the cubic:

$$\lambda^3 - [4 + (1-\nu^2)\Omega^2]\lambda^2 + [4 + (1-\nu)(1-\nu^2)\Omega^2 + (1+\xi)(1-\nu^2)(1-\Omega^2)]\lambda$$
$$+ (1-\nu)(1-\nu^2)\{\Omega^2 - 2/(1-\nu)\}\{1 + \xi(1+\nu)(\Omega^2 + 1/(1+\nu))\} = 0$$

In addition to the above, the membrane stress resultant, N, the moment resultant , M, and transverse shear resultant are given by Kalnins as

$$N = \frac{Eh}{(1-\nu)R}\sum_{\alpha=1}^{3} A_\alpha\{(1+\nu C_\alpha\lambda_\alpha)P_{n_\alpha} - (1-\nu)\cot\phi\, C_\alpha P'_{n_\alpha}\} \quad \ldots.(4)$$

$$M = \frac{D}{R^2}\sum_{\alpha=1}^{3} A_\alpha\{1+(1+\nu)C_\alpha\}\{\lambda_\alpha P_{n_\alpha} + (1-\nu)\cot\phi\, P'_{n_\alpha}\} \quad \ldots.(5)$$

$$Q = \frac{D}{R^3}\sum_{\alpha=1}^{3} A_\alpha\{1+(1+\nu)C_\alpha\}\{\nu+\lambda_\alpha-1\}P'_{n_\alpha} \quad \ldots.(6)$$

$$D = Eh^3/[12(1-\nu^2)]$$

(Note: Legendre functions appear with argument cos ϕ assumed)

If the components of the stiffness matrix of the support, referred to directions n and t of Figure 1, are Knn, Ktt and Knt (symmetric with Ktn] and K is the restoring moment per unit angular displacement, then the boundary conditions that stresses and moments are continuous across the boundary, yield the matrix equation in Aj:

$$\sum_{j=1}^{3} S_{ij}A_j = 0 \quad \ldots.(7)$$

where:

$$S_{1j} = \frac{2\pi D\sin\phi_0}{R^2}[1+(1+\nu)C_j](\nu+\lambda_j-1)P'_{n_j} - K_{nn}P_{n_j} + K_{nt}(1+\nu)C_j P'_{n_j}$$

$$S_{2j} = \frac{2\pi Eh\sin\phi_0}{(1-\nu)}\{(1+C_j\lambda_j)P_{n_j} + (1-\nu)\cot\phi_0 C_j P'_{n_j}\} - K_{tn}P_{n_j} + K_{tt}(1+\nu)C_j P'_{n_j}$$

$$S_{3j} = \frac{D}{R}\{2\pi\sin\phi_0[1+(1+\nu)C_j][\lambda_j P_{n_j} + (1-\nu)\cot\phi_0 P'_{n_j}]\} + \frac{1}{R}P'_{n_j}K$$

Meaningful solutions of (7) only exist when the determinant of S changes sign. Hence the modes of the spherical shell in are can be determined by stepping by small intervals over the desired range.

The Effect of Water Loading

It can be shown that the equation of motion of a spherical shell set in a matching sperical baffle can be written terms of the amplitudes, $\hat{a}_i$, of its in vacuo modes:

$$(\omega_i^2 - \omega^2)\hat{a}_i = \mathcal{F}_i - (\rho T^i)^{-1}\sum_{(j)}\hat{a}_j\int_S \hat{P}^j\hat{W}_i\, dS \quad \ldots.(8)$$

$$T^i = h\int_S(\hat{W}_i^2 + \hat{U}_i^2)\, dS$$

$\hat{P}_j$ is the radiated pressure field due to exciting the jth mode with unit amplitude. Integration is carried out over S, surface area of the shell.

$\mathcal{F}_i$ is a generalised forcing term related to the actual driving force density $\hat{\underline{F}}$ according to:

$$\mathcal{F}_i = \frac{1}{(\rho T^i)} \int_{\text{volume}} \hat{\underline{F}} \cdot \hat{\underline{x}}_i \, dV$$

where $\hat{\underline{x}}^i$ is the ith mode displacement.

The form of radiated pressure field from a spherical source is known (e.g. Morse, 1948) and allows the integral on the RHS of eqn 8 to be replaced by

$$\int_S \hat{p}^j \hat{w}_i \, ds = 2\pi R^2 \sum_{m=0}^{\infty} \sum_{\alpha,\beta=1}^{3} D_m A^j_\alpha A^i_\beta S_{n^j_\alpha, m} S_{n^i_\beta, m} \quad \ldots\ldots(9)$$

where A^j_α = the set of A_α coefficients of the j^{th} mode

$$S_{n,m} = \int_0^{\beta_c} P_n(\cos\phi) P_m(\cos\phi) \, d(\cos\phi); \quad D_m = -\frac{\sigma c (m+\frac{1}{2}) \omega h_m(\mu)}{h'_m(\mu)}$$

where σ is the density of water, C the speed of sound in water , is the wave number and $\mu = KR$

h_m is the hankel function and the prime denotes its derivative.

Note that a uniformly applied pressure driving force allows $\mathcal{F}_i$ to be represented by

$$\mathcal{F}_i = (\rho T^i)^{-1} \sum_{\alpha=1}^{3} A^i_\alpha S_{0, n^i_\alpha}$$

The modal coefficients, $\hat{a}_i$, if known, can then be used to calculate power radiated and radiated pressure fields using standard expressions (eg Morse 1948)

Truncation of Modes and Water Pressure Terms

Equation (8) represents an infinite number of equations, each having an infinite sum on the RHS. The arguments as to how many modes should be included are complex and are not presented here. Suffice it to say that, for the present work, 3 modes were accounted for.

Truncation is again required for the integral term (eqn 9) and the criterion adopted there was that m should exceed the maximum value of n^j_α

Determination of Support Stiffness

Diagram (2) illustrates the support and spherical cap actually used in this study. The transducer was examined with the support in 5 different cases;

1) All elements present

2) Element 1 missing

3) Elements 1,2 missing

4) Elements 1,2,3 missing

5) Elements 1,2,3,4, missing

The stiffnesses were determined by finite element analysis a description of which is given adequately elsewhere (PAFEC Manual 1976).

RESULTS

The partial sphere transducer studied had a radius of curvature, 48mm, thickness 1mm and semicap angle 14.72^{o}. The material used was PZT4 which has a Young's modulus of 8.13×10^{10} and Poisson's ratio 0.329. The geometry of the mounting for the transducer has already been described in the previous section. Table 1. gives the stiffnesses for the five cases studied.

Figure 3. shows a plot of $\log_{10}|S|$, S being the matrix, S, of equation(11), against dimensionless frequency Ω for case 1. Three modes are indicated in the range $0<\Omega<10$ Care must be taken not to take the point that $|S|$ changes from imaginary to real as a mode: it is not.

Table 2. shows the predicted frequencies and the actual frequencies measured in air. Agreement is good for mode 1 and the one example of mode 2. In mode 3 the predicted frequency is high by a factor of just over 4%. This arises because ω approaches the lowest natural frequency of the support and it is no longer sufficient to consider the static stiffness.

The shapes of the three modes for case 5 are shown in Figure 4. The figure justifies the earlier assumption that the tangential component of displacement may be neglected for the 1st three modes. For the most part, the tangential component is well under $^{1}/_{10}$th the normal component of displacement.

Table 3. shows predicted and actual frequencies for water loading. In all cases 40 pressure terms were considered. The predicted reductions in frequencies of the 3 modes are respectively 4.1, 5.8 and 8.5 kHz compared with actual reductions of 3.1, 5.5 and 3.8.

The differences in the results have almost certainly arisen because of experimental error of determinining the resonances in water and, further, that the actual transducer was not set in a spherical baffle. Therefore theoretical boundary conditions were not replicated exactly.

Figure (5) shows the variation of pressure, on the axis of symmetry of the transducer, with frequency as predicted by the theoretical model for 20 and 40 pressure terms and as obtained experimentally. The figure indicates good agreement between the model and experimental, the principal differences arising because of the slight differences in predicted and actual resonant frequencies.

CONCLUSION

The results indicate that the model for predicting the modes and their frequencies in air is particularly reliable, the differences between predicted and practical measurement in the case studied nowhere exceeding 1.5%. Even in water, the differences that do arise are attributable to the application of different boundary conditions in the theoretical and experimental cases. This difficulty could be resolved by one of two ways:

a) To simulate mathematically the actual boundary of the transducer and support of the transducer. This, however, poses analytical difficulties arising from mixed boundary value problems.

b) To set the experimental transducer in as near perfect a spherical baffle as possible.

It is unfortunate that the easiest case to deal with analytically is the most difficult to set up experimentally but it would appear to be the only feasible way at present.

Finally, an important and interesting result is that only two modes bracket any frequency of interest need be considered for transducers of mass and stiffness characteristics comparable with those considered her; this is condition satisfied by most transducers.

REFERENCES

Kalnins A.(1964) J. Acoust. Soc. Amer. 36(1), 74-81

Lou, Y.K. and Su, T.C.(1978) J. Acoust. Soc. Amer. 63(5), 1402-08

Morse PM(1948) 'Vibrations and Sound' McGraw-Hill Book Company, Inc.

The PAFEC Manual 'PAFEC75 Easidata' (1976)

Sonstegard DA(1969) J. Acoust. Soc. Amer. 45(2), 506-510

TABLE 1

Case	Krr $X10^{-9}$	Kzz $X10^{-9}$	Krz $X10^{-9}$	KzR $X10^{-9}$	K $X10^{-3}$
1	1.557	3.108	-.746	-.680	1.808
2	.887	2.673	-.269	-.295	1.621
3	.525	1.398	.114	.111	.289
4	.305	1.370	.137	.132	.080

Table of Support Stiffnesses in SI Units

TABLE 2

Case	Mode 1	Mode 2	Mode 3
1	16.93(16.74)	42.02	90.63
2	16.30(16.07)	41.93	90.57
3	15.17(15.16)	41.06	88.61
4	14.85(14.79)	40.96	88.51
5	14.19(14.02)	40.59(40.45)	88.01(84.28)

Table of frequencies (kHz) of the first three modes in air. Experimental values, where available, are in parenthesis.

TABLE 3

Case	Mode 1	Mode 2	Mode 3
1	12.4(12.6)	-	-
2	12.0(12.1)	-	-
3	11.o(11.2)	-	-
4	10.8(11.3)	-	-
5	10.1(10.9)	34.8(34.1)	79.5(80.3)

Table of frequencies (kHz) of the first three modes in water. Experimental values are in parenthesis.

LEGENDS

Figure 1. Geometry of the shell

Figure 2. Geometry of the support

Figure 3. Variation of $|S|$ with dimensionless frequency, Ω. Three resonances are indicated by arrows

Figure 4. The shapes of the first three modes

Figure 5. Variation of Pressure at 1 m from the transducer on the axis of symmetry.

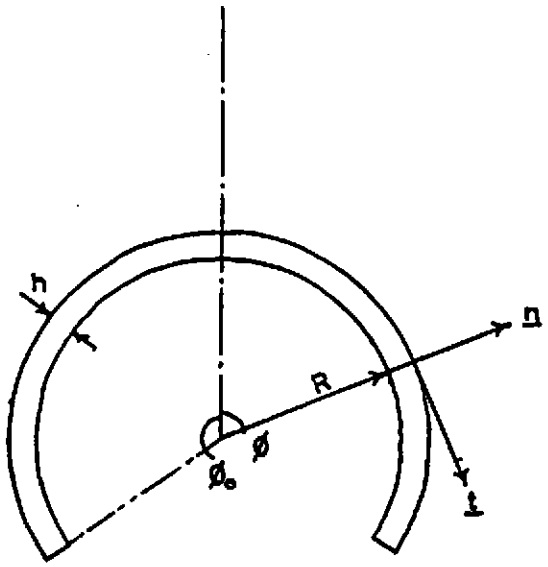

figure 1

figure 2

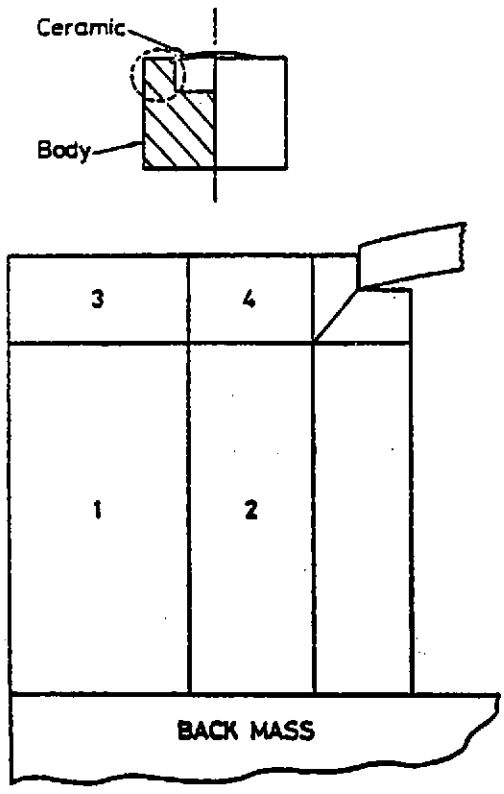

FINITE ELEMENT MODEL

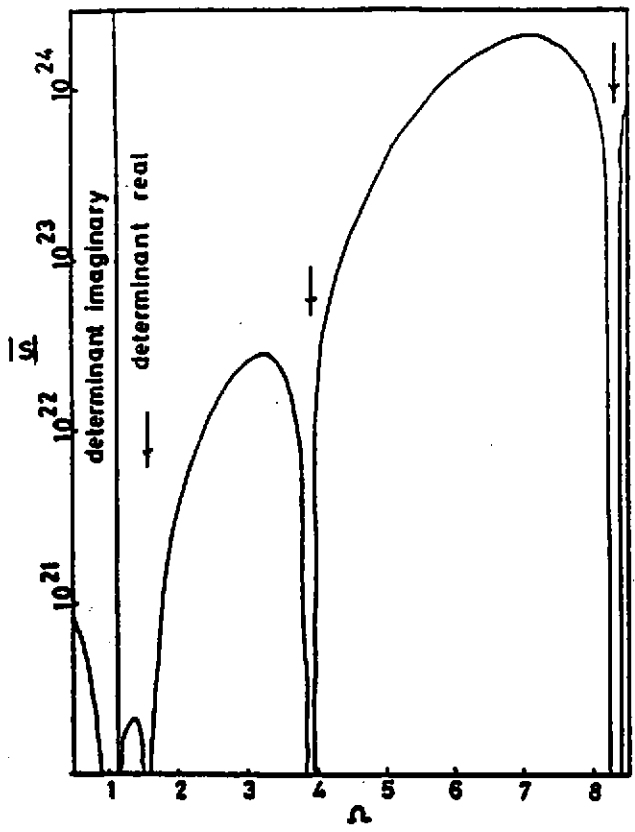

figure 3

figure 4

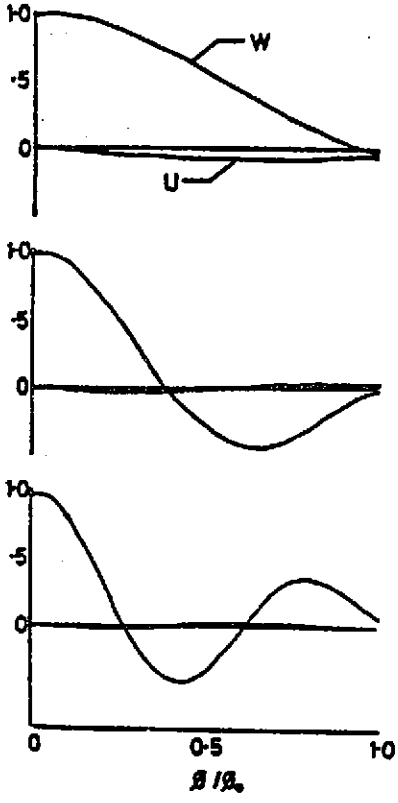

figure 5